

Received 6 November 2024, accepted 27 November 2024, date of publication 2 December 2024, date of current version 10 December 2024.

Digital Object Identifier 10.1109/ACCESS.2024.3509643

RESEARCH ARTICLE

Engine Oil Quality Monitoring Using an Additively Manufactured X-Band Microwave Waveguide Sensor

YOUNESS ZAAROUR¹, (Student Member, IEEE),
JUAN LUIS CANO², TOMAS FERNANDEZ², (Member, IEEE),
FATIMA ZAHRAE EL ARROUD¹, (Student Member, IEEE),
ABDESSAMAD FAIK³, RAFIQ EL ALAMI¹, AND HAFID GRIGUER¹, (Member, IEEE)

¹Microwave Energy Sensing (MES), Digital Innovation Center of Excellence (DICE), University Mohammed VI Polytechnic, Ben Guerir 43152, Morocco

²Departamento de Ingeniería de Comunicaciones, Universidad de Cantabria, 39005 Santander, Spain

³Laboratory of Inorganic Materials for Sustainable Energy Technologies (LIMSET), University Mohammed VI Polytechnic, Ben Guerir 43150, Morocco

Corresponding author: Youness Zaarour (youness.zaarour@um6p.ma)

This work was supported by the Ph.D. Student Grant from the University Mohammed VI Polytechnic (UM6P).

ABSTRACT Maintaining engine oil quality is critical for industrial machinery and transformers to ensure efficient operation and reduce the risk of failure. This paper presents a novel application of an X-band microwave sensor, using a third-order electroformed iris waveguide filter, for real-time, non-invasive engine oil quality monitoring. By detecting shifts in the dielectric properties of engine oil, the sensor accurately tracks oil degradation as it ages. Unlike traditional methods that require oil extraction and laboratory analysis, this sensor enables continuous, in-situ monitoring, providing immediate feedback without disrupting system operations. Any change in oil quality causes a frequency shift, as variations in its dielectric properties affect the waveguide's resonance. This shift can be measured in real time, enabling accurate monitoring of oil degradation. Additional measurements were conducted using the coaxial probe technique to analyze the changes in the oil's electrical behavior during various heating periods. Experimental results demonstrate the sensor's sensitivity, with measurable frequency shifts of up to 10 MHz observed in the most aged oil samples. These shifts clearly correlate with the oil's aging process, confirming the sensor's potential for practical use in predictive maintenance. This system, utilizing an electroformed waveguide, offers a cost-effective and efficient solution for enhancing machinery longevity and optimizing maintenance schedules in industrial applications.

INDEX TERMS Engine oil quality monitoring, microwave sensor, X-band, waveguide, permittivity, frequency shift, S-parameter, 3D printing, electroforming, conductive coating.

I. INTRODUCTION

The aging of engine oil in industrial transformers critically impacts performance and reliability, often leading to reduced efficiency, higher maintenance costs, and potential failures [1], [2], [3]. As oil deteriorates, its insulation properties weaken, increasing the risk of overheating and short circuits. To address this, predictive maintenance strategies are essential [4], [5]. By continuously monitoring oil quality

The associate editor coordinating the review of this manuscript and approving it for publication was Li Yang¹.

with advanced sensors, early signs of degradation can be detected, allowing for timely maintenance. This proactive approach not only prevents unexpected failures, but also extends the lifetime of the transformer and reduces costs, ensuring optimal operation and reliability [6].

Despite the importance of this monitoring, current techniques face several challenges. Traditional methods for assessing engine oil quality, such as chemical analysis and laboratory testing, are typically costly, time-consuming, and often require operational shutdowns and sample transportation, leading to interruptions and delays [7], [8]. Various

methods for assessing the quality of engine oil have been introduced in the literature [9], [10], [11].

These methods are also invasive and necessitate extensive sample preparation, which limits their practicality for real-time monitoring in industrial settings. In this context, microwave sensing technology emerges as a powerful alternative. It offers a non-invasive, real-time, and cost-effective way to analyze the dielectric properties of materials through their interaction with electromagnetic waves. This approach has been successfully applied in various applications, including medical diagnosis [12], [13], [14], Food control [15], [16], industrial processes [17], [18], and chemical production [19]. By detecting changes in the dielectric constant, microwave sensors offer immediate and precise evaluations with the capability to be seamlessly integrated into existing systems for continuous inline monitoring. This integration is particularly advantageous for preventing unplanned downtimes and improving the overall reliability of industrial operations. For example, in the analysis of edible oils [20], single-port submersible resonators have been used to determine the heating duration by measuring frequency shifts. However, the microstrip technology used in these sensors can be vulnerable to electromagnetic interference. Furthermore, while a non-intrusive microwave sensor has been suggested for detecting oil adulteration [21], its surface-focused microstrip resonator design primarily interacts with the material directly adjacent to the sensor, potentially limiting its effectiveness in bulk oil sample analysis.

A novel solution to these challenges lies in the use of waveguides, which provide a robust medium that effectively supports and confines electromagnetic waves, reducing interference susceptibility. Waveguides also maintain a high electric field, improving sensitivity and accuracy, especially for bulk sample analysis [22]. To the best of our knowledge, this is the first time a waveguide will be proposed for engine oil quality detection in the literature, marking a significant advancement in microwave sensing technology. Considerable research has been dedicated to utilizing waveguides for microwave sensing in various applications. For example, in [23], a study used a Ku band waveguide to detect ice accumulation on metallic surfaces from a distance, with sample volumes between 100 μL and 400 μL . This detection was achieved by observing a 170 MHz shift in the resonance frequency of the S11 parameter, demonstrating the waveguide's sensitivity to surface changes. In [24], another study employed a WR62 waveguide for measuring the flow rate of uniform liquids, detecting changes in the liquid's dielectric properties due to variations in heat exposure time. Additionally, in [18] an X-band waveguide was used as a proof of concept for gas sensing. In this case, an aerogel was exposed to air or a moderate vacuum, resulting in a 3 dB change in signal magnitude. In [25], a mid-infrared sensor platform using FT-IR and hollow waveguides enables real-time detection of NO, NO₂, and N₂O, providing high sensitivity with detection limits of

10, 1, and 0.5 ppm, respectively, for vehicle exhaust monitoring.

The working principle behind these approaches relies on the fact that changes in the material, such as alterations in composition, temperature, or other physical properties, can affect its dielectric characteristics. These changes, in turn, cause variations in the behavior of the electromagnetic waves, leading to shifts in frequency, phase, or amplitude after interacting with the material under test (MUT). Specifically, the phase constant β and attenuation constant α , which represent the rate at which the phase and amplitude of the wave change as it propagates through the material, are influenced by these dielectric properties.

To provide a more accurate representation for the attenuation constant, we use the following expression:

$$\alpha = \omega \sqrt{\mu \epsilon} \left\{ \frac{1}{2} \left[\left(\frac{\sigma}{\omega \epsilon} \right)^2 + 1 \right]^{1/2} - \frac{1}{2} \right\}^{1/2} \quad (1)$$

Under the condition of a good conductor, where the conductivity σ is much larger than the product of angular frequency ω and permittivity ϵ , i.e., $\left(\frac{\sigma}{\omega \epsilon} \right)^2 \gg 1$, this expression simplifies to:

$$\alpha \approx \sqrt{\frac{\omega \mu \sigma}{2}} \quad (2)$$

Following a similar procedure, the phase constant can be approximated by:

$$\beta \approx \sqrt{\frac{\omega \mu \sigma}{2}} \quad (3)$$

These simplified equations apply in this case because both the phase constant β and the attenuation constant α are determined primarily by the material's conductivity and the frequency of the wave [26].

These variations in phase and amplitude are detected by the sensor and converted into measurable signals, providing immediate feedback on the condition or quality of the material. Despite the considerable potential of microwave sensing, its practical application for engine oil analysis has not been fully explored. One major limitation in the current literature is that most sensors are designed to be in direct contact with the oil, which poses a risk of contamination or damage to the sensor over time. This direct exposure can lead to sensor degradation, reduced accuracy, and higher maintenance costs. In this work, we introduce the design and implementation of an X-band third-order iris filter waveguide specifically optimized for engine oil quality monitoring. Unlike previous studies, such as [24], which used an aluminum WR-62 waveguide with irises added separately for flow rate measurements, our approach takes a significant step forward by employing a precisely engineered seamless iris filter waveguide. This single-unit design not only improves measurement accuracy and reliability but also avoids direct contact with the oil by incorporating a dedicated channel for importing the material under test, thereby protecting the sensor and enhancing its durability.

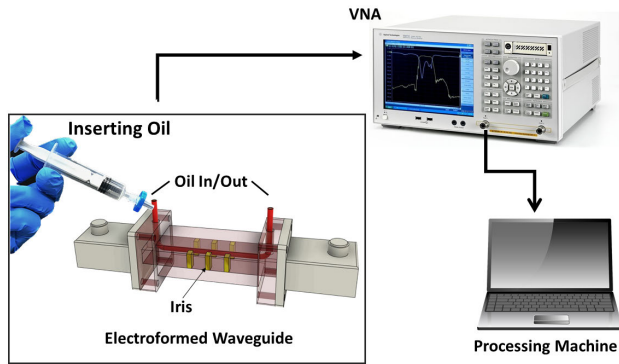


FIGURE 1. Detailed illustration and explanation of the operating process of the proposed microwave sensor.

This paper demonstrates the effectiveness of an electroformed waveguide sensor in detecting changes in oil properties caused by varying heating durations, proving to be a reliable tool for monitoring oil aging by identifying these variations. The sensor’s preparation and fabrication process are detailed in Section II-A, while Section II-B describes the sensing methodology and provides an analysis of the sensor’s microwave responses to oils with different aging profiles. Section III explores the dielectric behavior of engine oil through complex permittivity measurements using the coaxial probe technique. Finally, Section IV presents the conclusions, summarizing the sensor’s reliability in detecting oil aging.

II. OIL QUALITY SENSOR: DESIGN AND ANALYSIS

A. DESIGN AND FABRICATION

The sensor design features a WR90 waveguide integrated with three pairs of rectangular half-wavelength resonators operating in TE₁₀ mode. These resonators are separated by inductive irises, with each pair positioned $d = 9$ mm apart. These irises act as impedance inverters, symbolized by K_{01} , which represents the specific coupling coefficient for the fundamental TE₀₁ mode in the waveguide. K_{01} is oriented by the following equation:

$$Z_{in} = \frac{K_{01}^2}{Z_L} \quad (4)$$

where Z_L and Z_{in} are the load and input impedance of the K_{01} block respectively.

$$\frac{K_{01}}{Z_0} = \sqrt{\frac{\pi}{2} \frac{(f_2 - f_1)}{2g_0g_1\omega_1}} \quad (5)$$

f_0 is the resonance frequency of the band-pass filter, and f_c is the cutoff frequency for the TE₁₀ mode. The parameters g_0 , g_1 , and ω_1 are related to the prototype parameters of the low-pass filter, while $f_2 - f_1$ indicates the 3 dB bandwidth of the filter around the resonance frequency f_0 [27]. The selection of the WR90 waveguide and the corresponding frequency range around 11 GHz was largely influenced by the equipment available in our laboratory, as it allows us to efficiently utilize

existing resources and components for a timely, cost-effective fabrication process. This configuration is optimized for a target center frequency of approximately 11 GHz, which aligns with our experimental requirements and provides the necessary sensitivity and resolution for detecting changes in the material properties. Fig. 1 illustrates the proposed engine oil sensing process employing the electroformed waveguide.

The waveguide, meticulously designed using ANSYS HFSS, achieves a high Q factor of around 244 and a narrow bandwidth of 0.4%. The optimized structure, as shown in Fig. 3(a), include a rectangular aperture with a height of $b = 10.16$ mm and a width of $a = 22.86$ mm and a total length of 80 mm. Each iris has a width of $c = 3$ mm and a length of $e = 5.64$ mm, forming resonant cavities essential for filter performance. To facilitate oil flow inside the filter, two holes with a radius of 5.2 mm are incorporated on each side of the waveguide, supporting a tube channel with an inner diameter of 4.8 mm and an outer diameter of 5 mm. The tube is made of silicone, which has a permittivity of $\epsilon_r = 2.9$.

The waveguide is fabricated using a 3D resin printer (EPAX X1-N) with a resin material of dielectric constant 2.9 and loss tangent 0.004, printed with an infill density of 1 to ensure structural integrity and minimize air gaps. After printing and cleaning, an initial conductive layer is applied by coating the waveguide with a conductive silver spray, which has a conductivity of 1×10^5 S/m. This layer ensures uniform conductivity throughout the surface, which is essential for the subsequent electroforming process. The waveguide then

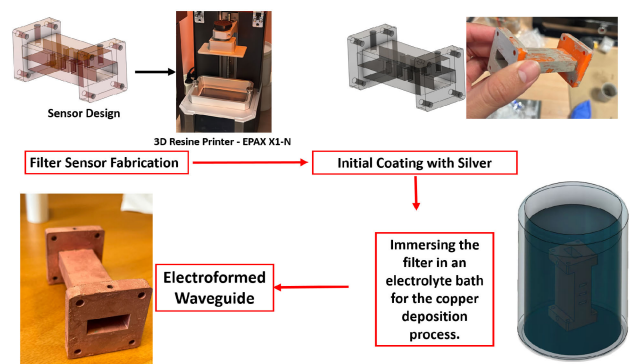


FIGURE 2. Step-by-step illustration of the Electroformed iris filter fabrication process using 3d printing and electroplating techniques.

undergoes copper deposition by being immersed in an electrolyte bath containing a copper sulfate solution for about 30 minutes, where it is connected to a power supply to create an electrochemical reaction that deposits copper onto the silver-coated surface. The process is meticulously controlled to achieve a uniform copper layer with a thickness of 20 μm , which enhances the waveguide’s electrical conductivity and mechanical strength. One of the challenges during the electroforming process was ensuring even copper deposition across the waveguide’s complex surface. This issue was addressed by precisely regulating the electrolyte composition and adjusting the power supply to maintain a consistent current density (Fig. 2).

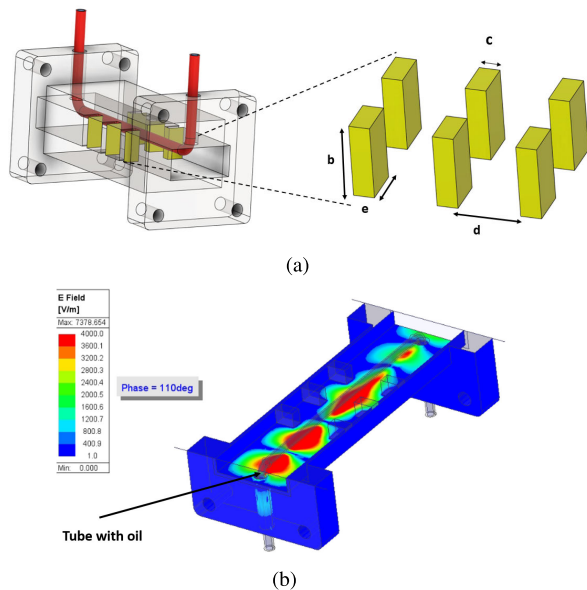


FIGURE 3. (a) Schematic and electroformed fabricated waveguide with internal structure and physical prototype (b) H-Plane cross-section of the iris filter waveguide showing an intense E-field.

B. WAVEGUIDE SENSING METHODOLOGY

The main concept of this application involves the use of a waveguide filter iris that excites the TE_{10} mode, where the electric field (E-field) is most intense in the mid-plane along the wide dimension. To enhance interaction with this region, a tube channel is inserted in direct contact with the high-field area (Fig. 3(b)), ensuring maximum sensitivity and precision in detecting small variations in the dielectric properties of engine oil passing through the tube. This direct contact configuration establishes the sensor as a contact-type device, enabling effective material sensing through close interaction with the E-field.

Changes occurring in the environment between the three iris pairs can lead to variations in the resonant amplitude and resonant frequency of the structure. Altering the permittivity through the resonators can modify f_0 . When all variables in (5) are kept constant, a change in f_0 will result in a change in K_{01} . According to (4), this variation in K_{01} affects the impedance observed from the input of the impedance inverter block. Consequently, changing the permittivity in the center of the resonator alters its f_0 and the input impedance at the iris and waveguide junction. These impedance variations can be monitored using $|S_{11}|$ (dB) from the waveguide input. As a result, the S_{11} simulation presented in Fig. 4(a) demonstrates that changes in the permittivity of the medium lead to a noticeable shift in the resonant frequency. This indicates that perturbations in the medium between the three pairs of irises directly affect the resonant frequency of the filter, emphasizing its sensitivity to the dielectric properties of the medium.

The S-parameters of the proposed iris filter were measured in a frequency range of 8.5 to 12.5 GHz using a vector network analyzer E8364A from Agilent. Prior to measurement, a two-port TRL (Thru-Reflect-Line) calibration was

performed to ensure accuracy. The reflection coefficients, both simulated and measured, are presented in Fig. 4(b). As depicted in the figure, the simulated results closely align with the measured data in terms of frequency. However, there is a magnitude difference of approximately 23 dB, which can be attributed to the increased surface roughness and lower electrical conductivity compared to the theoretical values. This agreement between simulation and measurement, despite the noted discrepancy in magnitude, validates the design approach and highlights the impact of manufacturing processes on the filter's performance. The VNA was configured to operate with an output power of 0 dBm, an IF bandwidth of 100 Hz to reduce noise, and 4501 sweep points. While VNAs like the E8364A excel in capturing precise S-parameters in controlled settings, they are costly and complex for real-time, in-field liquid monitoring. More practical alternatives for real-time applications include custom microwave sensors, portable network analyzers, or RF modules like Software Defined Radios (SDRs), which offer simplified, cost-effective measurement capabilities. This study establishes foundational insights, with future work focusing on adapting these findings to practical, real-time monitoring systems.

The first measurement to prove the sensitivity of the set-up was carried out using a 12 cm plastic tube filled with distilled water at a controlled room temperature of 26 °C. A syringe was used to fill the tube with water, with an outlet for managing waste. The tube was securely fixed to the waveguide with permanent Scotch tape to prevent movement and ensure repeatable measurements. The volume of water inside the tube was approximately 3.45 ml. To ensure a static measurement, the readings were taken once the flow had ceased and the liquid was stable. The reflection coefficient $|S_{11}|$ of the fabricated iris waveguide was measured for three scenarios and is shown in Fig. 4(c). These scenarios include an unloaded waveguide with a resonant band-pass at 11.29 GHz, a waveguide with an empty tube, and a waveguide with a water-filled tube.

The results indicate that the water-filled tube caused a significant shift in the resonance frequency by approximately 950 MHz and an amplitude change of -5.4 dB, demonstrating the filter's sensitivity to changes in the dielectric properties of the medium inside the waveguide. Considering that the relative permittivity of water is approximately 80 (at room temperature and microwave frequencies), this substantial shift underscores the sensor's capability to detect variations in permittivity. Throughout the water measurements, the results demonstrated consistent repeatability of the sensor response across five measurement repetitions. After evaluating the sensitivity of the waveguide with water, we advanced to testing the method with engine oil used in a transformer and heated to 150 °C for different durations.

Next, we examined the impact of different oil samples with varying aging periods by monitoring the peak resonance frequency of the S_{11} parameter in the electroformed

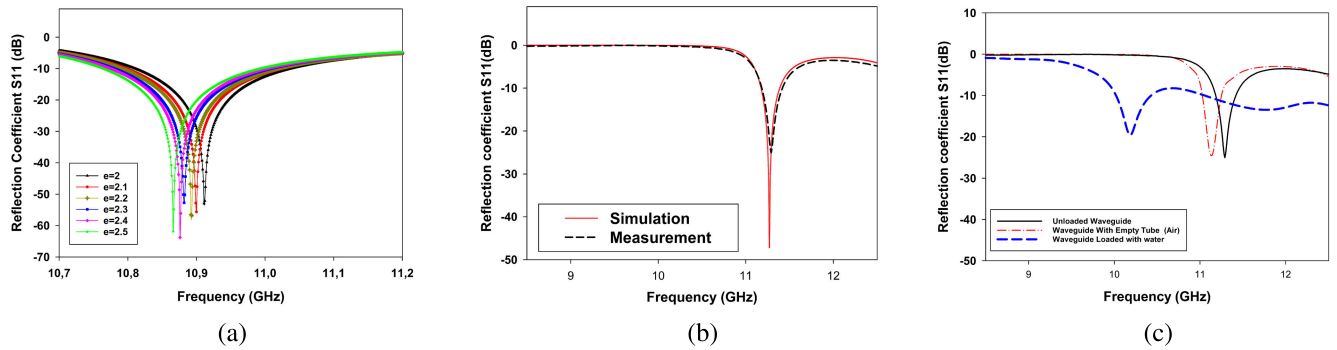


FIGURE 4. (a) Simulated reflection coefficient S_{11} of the waveguide for varying dielectric constants in the surrounding environment. (b) Simulated and measured parameter S_{11} of the proposed microwave sensor. (c) Simulated S_{11} for the unloaded waveguide, with the tube and loaded with water.

TABLE 1. Humidity levels and aging periods of various oil samples.

Oil Samples	Aging Period (h)	Humidity (ppm)
1	fresh oil	351.7
2	148	325.7
3	316	352.5
4	604	393.4

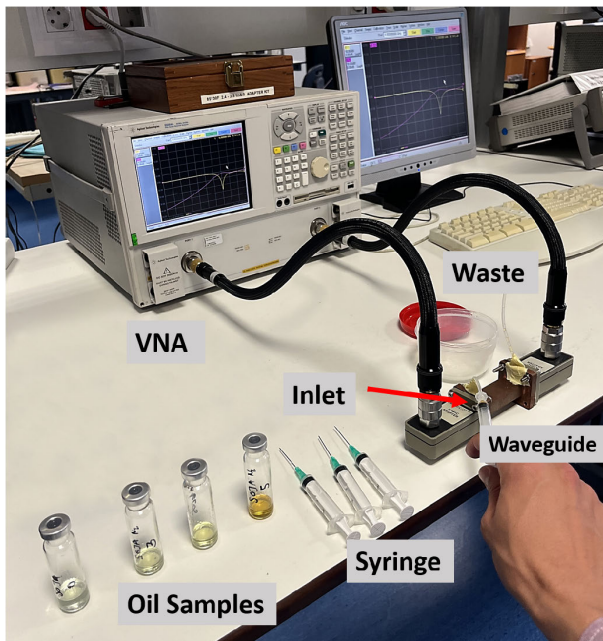


FIGURE 5. Experimental setup for engine oil controlling including the samples, the waveguide and the processing machine.

waveguide, using the setup presented in Fig. 5. The four samples of oil were stored in four different glass tubes, and four different syringes were used to insert each oil in the channel. For each oil sample measured, the tube was rinsed with distilled water to prevent any cross-contamination between samples. The resonance frequency shifts of the sensor are illustrated in Fig. 7, highlighting the sensor’s frequency response for each oil sample. As the period of oil usage increased, a corresponding decrease in the resonance frequency was observed. This decrease is caused by an increase in the oil’s dielectric constant and loss factor as a result of aging, as will be demonstrated in Section D. Over

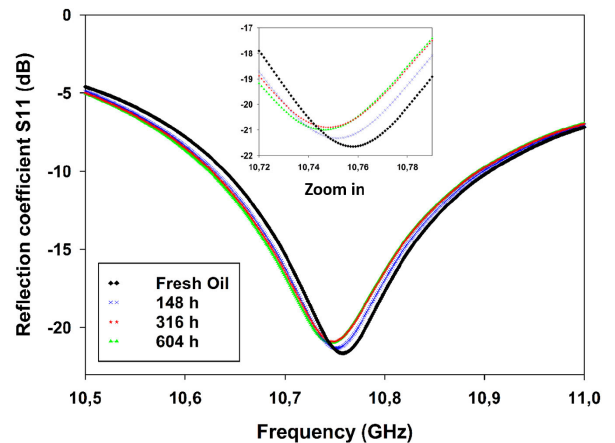


FIGURE 6. Measured S_{11} variation for different oil heating durations.

time, the chemical composition of the oil degrades, leading to changes in its dielectric properties, which in turn shift the resonance frequency, and this is confirmed by the complex permittivity measurement in the next section.

To monitor the quality of engine oil, we measured the sensor’s response by calculating Δf , which detects the relative frequency change for oil samples of varying age. Fresh oil serves as the reference point, and Δf is defined as:

$$\Delta f = f_{\text{Fresh oil}} - f_{\text{aged oil}} \tag{6}$$

where $f_{\text{Fresh oil}}$ represents the resonance frequency with fresh oil, and $f_{\text{aged oil}}$ corresponds to the resonance frequency with aged oil. This approach allows us to quantify the changes in the dielectric properties of the oil as it ages, once it is introduced into the sensor.

As seen in Fig. 6, the graph demonstrates the relationship between the aging period of oil and the corresponding frequency shift (Δf) detected by the sensor. A clear positive correlation is observed, with older oil samples causing more significant shifts in the sensor’s frequency response. The nonlinear trend, illustrated by the fitted line, indicates that the frequency shift accelerates with longer aging periods. This relationship can be quantitatively described by (7):

$$\text{Aging Period}_{\text{Measured}} = 5.094 \cdot (\Delta f)^2 - 4.952 \cdot (\Delta f) + 8.86 \tag{7}$$

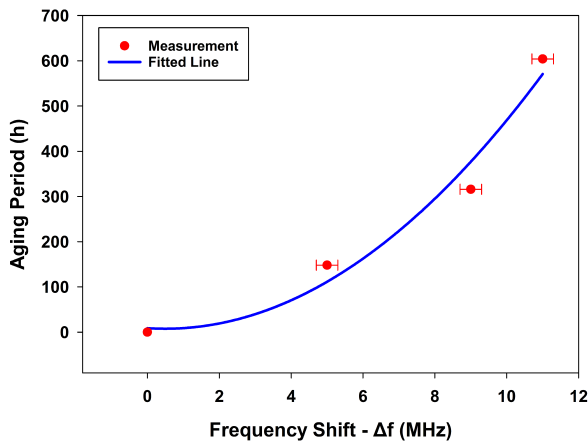


FIGURE 7. The aging period of oil compared to the changes in its resonance frequency (MHz).

Using (7), valuable insights into the oil’s aging process relative to the reference oil (fresh oil) can be derived. By measuring the frequency shift (Δf) of a given oil sample and applying the equation, the degree of aging of the oil compared to fresh oil can be determined. This allows for effective monitoring of oil quality and timely identification of when the oil, such as engine oil, needs to be replaced, ensuring optimal performance and longevity of the equipment. This model demonstrates the sensor’s capability to offer an accurate, non-invasive approach to evaluating oil degradation over time. The insights gained from this data can contribute to the creation of predictive maintenance models, enabling real-time monitoring of oil condition through resonant sensors.

The fitted function in Equation (7) was derived as an empirical model based on the measured data, accurately representing the correlation between the aging period and the frequency shift (Δf). This empirical relationship is consistent with the theoretical framework provided by Equation (9), which describes the complex permittivity ($\epsilon^*(f)$) of the oil as a function of frequency. Equation (9) captures the dielectric relaxation behavior of the material, with parameters like static permittivity and relaxation time reflecting the material’s response to applied electromagnetic fields. As oil ages, its dielectric properties undergo changes that influence the frequency response of the sensor, leading to a measurable frequency shift (Δf). Therefore, while Equation (7) empirically models the aging period, it indirectly reflects the underlying changes in dielectric properties as captured by Equation (6). This theoretical consistency reinforces the sensor’s effectiveness in tracking oil degradation, making it a valuable tool for applications requiring reliable, non-invasive monitoring of oil quality.

To ensure repeatability and reliability, each test was conducted multiple times under identical conditions. Measurements were repeated five times with the oil heated for 148 hours, and the standard deviation across trials was calculated to be 3%, demonstrating the sensor’s high consistency. This low level of uncertainty presented in Fig. 6

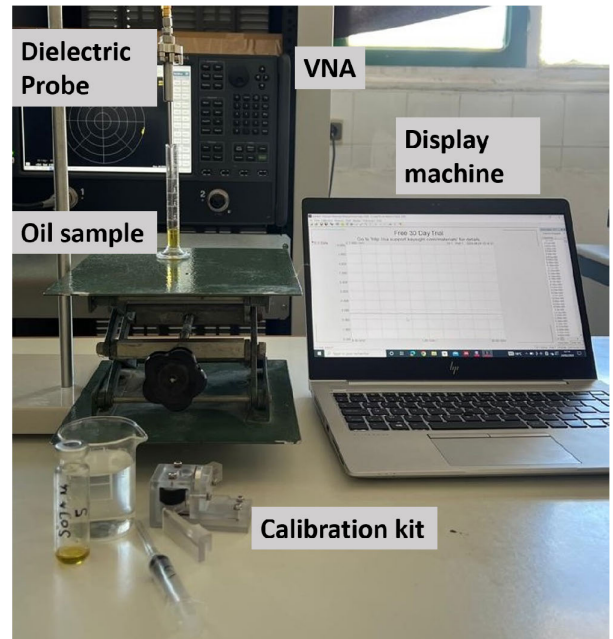


FIGURE 8. Experimental setup for measuring dielectric properties of oil samples.

confirms the consistency of the sensor’s performance, and the error bars visually illustrate the range within which the actual values are expected to fall, thereby validating the reliability of the measurement process.

III. ANALYSIS OF MEASURED DIELECTRIC PROPERTIES

To gain a deeper understanding of the relationship between the aging process and the frequency response, it is essential to examine the dielectric properties of the oil itself. By analyzing the complex permittivity, we can characterize how the material’s dielectric behavior changes with aging and affects the sensor’s readings. These dielectric properties are defined by two key parameters: the dielectric constant (ϵ') and the loss factor ($\tan \delta$), which together describe how the material interacts with electromagnetic fields.

This dependence of dielectric properties on frequency can be modeled using Debye’s relaxation model, which describes the frequency-dependent behavior of permittivity (f) [28]:

$$\epsilon^*(f) = \epsilon_\infty + \frac{\epsilon_s - \epsilon_\infty}{1 + j 2\pi f \tau} \tag{8}$$

where ϵ_s is the static permittivity (low-frequency limit), ϵ_∞ is the permittivity at infinite frequency, τ is the relaxation time, and f is the frequency.

This analysis of measured dielectric properties not only validates the sensor’s ability to detect changes in oil quality over time but also provides a theoretical basis for interpreting frequency shifts as indicators of aging. Understanding the dielectric response through Equation (6) further supports the empirical observations from Equation (5), establishing a comprehensive approach to real-time oil condition monitoring.

This method has been widely applied in dielectric spectroscopy over a broad frequency range for various

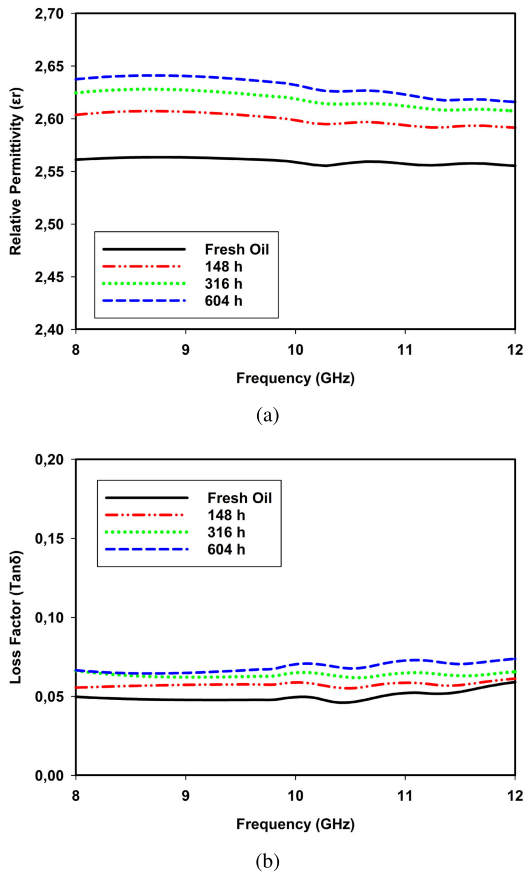


FIGURE 9. Measured complex permittivity of oil at four different aging period (a) Relative permittivity and (b) loss factor.

applications [29], [30], [31], [32]. The dielectric properties of oil at three different stages of use were measured using a Keysight N1501A-102 open-ended coaxial probe (Fig. 8). The parameters of the oil samples are listed in Table 1. To avoid contamination, the samples were stored in glass tubes. Furthermore, as shown by the humidity values in Table 1, the variation is negligible, ensuring that the results are correlated only with the aging period during high temperature.

The setup ensured precise and repeatable measurements by maintaining strict control over key variables such as sample volume, temperature, and humidity, effectively minimizing external factors that could influence the results. Measurements were conducted in a glass flask, ensuring consistent volume for each test to maintain repeatability. The coaxial probe was securely fixed using a bracket, while the flask was stabilized with a laboratory scissor jack to minimize cable movement and ensure consistency throughout the process. Calibration was performed using the short, load, and open standards from a calibration kit, and a reference measurement with water was taken to verify the accuracy of the setup. The measured results for the relative permittivity and loss factor in the 8-12 GHz range are shown in Fig. 9(a) and Fig. 9(b), respectively. For oil samples aged 148, 316, and 604 hours, the complex permittivity exhibited noticeable changes. The

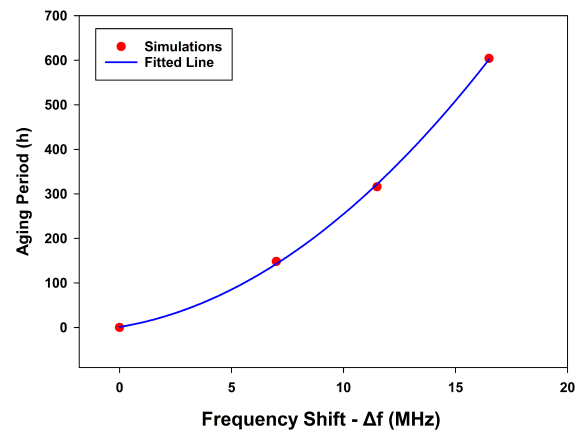


FIGURE 10. Simulated frequency shift Δf response for oil samples at varying freshness levels (Fresh Oil, 148 h, 316 h and 604 h).

relative permittivity of fresh oil begins at approximately 2.55 and gradually increases to around 2.65 after 604 hours of use. Similarly, the loss factor of fresh oil starts at about 0.05 and rises to approximately 0.1 after 604 hours. These results indicate clear shifts in both the relative permittivity and loss factor as the oil ages, confirming that the oil’s dielectric properties are influenced by prolonged use and exposure to high temperatures. The observed changes in dielectric properties reflect the degradation of the oil over time, validating the effectiveness of the sensor in monitoring oil aging. The measurement technique employed in our study effectively captures the frequency shifts and changes detected by the microwave sensor, which are directly linked to variations in the oil’s dielectric properties.

$$\text{Aging Period}_{\text{simulated}} = 1,2174 \cdot (\Delta f)^2 + 8,311 \cdot (\Delta f) + 11,925 \quad (9)$$

To further support our findings, we used Ansys HFSS (High-Frequency Structure Simulator) to simulate the oil-filled waveguide cavity, assigning the corresponding measured permittivity values for each aging period. We modeled the waveguide structure exactly as it was used in our experiments, ensuring the simulation closely matched the real measurement setup. The frequency shifts were calculated by observing changes in the extracted S_{11} reflection coefficient, which is sensitive to variations in the oil’s complex permittivity. Fig. 10 illustrates the relationship between the simulated frequency shifts and the aging period of the oil. The simulation shows a trend similar to that in the measured data, with higher frequency shifts as the oil ages. However, the measured frequency shifts (Fig. 7) are lower than those obtained from the simulations. To quantify the difference between the simulation and measured results, we use the Root Mean Square Error (RMSE) as a metric. RMSE is a commonly used measure of the differences between values predicted by a model and the values actually

TABLE 2. Sensitivity comparison of different frequency-shift.

Ref	Used Freq (GHz)	Type of Sensor	S_{av} %	ϵ_r Range
[33]	1.156	Planar SSR Filter	0.06	1-80
[34]	0.87	Planar SSR Filter	0.091	20-80
[35]	5.209	Planar SSR Filter	0.03	1-20.7
[36]	2.5	SIW Filter	0.066	1-77
[24]	16	Waveguide	2.16	1-3
This work	11.13	Waveguide	2.17/0.11	1-2.1/1-80

observed. It is defined as:

$$RMSE = \sqrt{\frac{1}{n} \sum_{i=1}^n (S_{11, \text{simulated}, i} - S_{11, \text{measured}, i})^2} \quad (10)$$

where $S_{11, \text{simulated}, i}$ represents the simulated S_{11} values, $S_{11, \text{measured}, i}$ represents the measured S_{11} values, and n is the number of data points. By using the RMSE metric, we find that the RMSE between the simulated and measured results is 3.18. This relatively low RMSE indicates that the simulation aligns quite well with the measured data, suggesting that the simulation model is reasonably accurate. However, the differences can still be attributed to fabrication imperfections and the use of additive manufacturing techniques, which may introduce surface roughness and reduce the conductivity of the waveguide material. This demonstrates the sensor's capability to monitor oil degradation accurately over time, making it a reliable method for assessing the aging process of oil through its dielectric behavior, particularly for detecting small shifts in the quality of oil with dielectric properties around 2.4, even with minor changes. These findings highlight the potential of this approach for real-time monitoring of oil quality and degradation. Using additive manufacturing for waveguides as a substitute for CNC manufacturing further enhances this method by offering more flexibility of design and cost efficiency. However, the aim of this paper is to show the validation of the approach rather than optimizing the sensitivity. It is interesting to mention that the Order 3 waveguide we made, with an 8 cm length, is not set to be the optimum. However, to increase sensitivity, we can extend the waveguide length and the order of the irises, creating more electric fields, thus providing a more sensitive measure of oil degradation. Finally, we compare our proposed sensor with existing studies. Because oil sensors often have different detection objectives, making direct comparisons difficult, we selected related fluidics sensors for a more meaningful assessment. It's important to point out that these sensors operate across different frequencies and accommodate varying ranges of permittivity changes. The details of this comparison are summarized in Table 2. The sensitivity is defined as the ratio of the frequency shift, Δf , to the change in permittivity. The relative average sensitivity is then obtained by normalizing the sensitivity with $f_{0, \text{air}}$, which is the sensor's resonance frequency in the absence of any material loading, and it is expressed as a percentage (%).

$$\bar{S}_{av} = \frac{S_{av}}{f_{0, \text{air}}} = \frac{\Delta f}{\Delta \epsilon_{MUT} * f_{0, \text{air}}} \% \quad (11)$$

Compared to other technologies, where planar SRR filters are primarily used at lower frequencies, our proposed sensor stands out by performing well across both low and high permittivity ranges. Additionally, the sensor's performance can be further enhanced by increasing the number of irises and optimizing the quality factor. Moreover, our work takes advantage of the waveguide's properties, ensuring that the sensor is resistant to external interferences, making it a robust option for reliable sensing.

IV. CONCLUSION

A novel non-intrusive technique for monitoring oil quality has been introduced, employing electroforming to create a cost-effective, lightweight, and highly sensitive waveguide iris. The results from the proposed setup demonstrated that the resonance frequency is responsive to changes in the oil's aging period, providing a clear indication of its quality. The sensor successfully detected frequency shifts in oil samples aged 148, 316, and 604 hours, compared to a fresh sample. This flexible and robust design shows scalability for a variety of quality monitoring applications, such as liquid concentration analysis or agricultural uses, where intrusive methods are undesirable.

In addition to oil quality monitoring, this sensor has the potential to be adapted for a range of other applications requiring non-intrusive liquid analysis. For example, it could be utilized to monitor chemical concentrations in industrial processes or detect impurities in water treatment facilities. This study has demonstrated a proof of concept for a robust and scalable microwave sensor capable of monitoring engine oil quality. While the sensor shows promising potential, challenges remain, particularly in terms of power consumption for extended in-field applications and the need for precise calibration in varying environmental conditions. Future work will focus on optimizing the waveguide design and incorporating AI-driven solutions to address these limitations. By leveraging machine learning for adaptive calibration and signal processing, the sensor's reliability can be further enhanced, ensuring accurate performance in dynamic environments. Additionally, AI-based power optimization could enable the sensor to adjust its energy usage dynamically, improving efficiency for continuous, real-time monitoring. With the foundational sensing mechanism now established, further development will focus on advancing the system towards a fully operational real-time application. Beyond the enhancements discussed, the test setup could be adapted to operate at lower frequencies, where affordable, portable vector network analyzers (VNAs) are available up to 6 GHz, making the system more accessible and cost-effective. These advancements have the potential to significantly improve the sensor's energy efficiency, scalability, and adaptability, positioning it to meet the rigorous demands of real-world applications. We anticipate expanding the applicability of this technology to various sectors that require precise and continuous monitoring of liquid properties, thereby broadening its impact.

ACKNOWLEDGMENT

The authors acknowledge the collaboration with Departamento Ingeniería de Comunicaciones (DICOM) for providing the facilities and Profs. Fernando Delgado and Profs. Cristian Olmo from the Department of Electrical and Energy Engineering, University of Cantabria for supplying the oil samples.

REFERENCES

- M. R. Meshkatodd and S. Abbaspour, "Aging study and lifetime estimation of transformer mineral oil," *Amer. J. Eng. Appl. Sci.*, vol. 1, no. 4, pp. 384–388, Apr. 2008.
- J. Liu, H. Zhang, C. Geng, X. Fan, and Y. Zhang, "Aging assessment model of transformer insulation based on furfural indicator under different oil/pressboard ratios and oil change," *IEEE Trans. Dielectr. Electr. Insul.*, vol. 28, no. 3, pp. 1061–1069, Jun. 2021.
- M. A. Mehmood, J. Li, F. Wang, Z. Huang, J. Ahmad, and M. S. Bhutta, "Analyzing the health condition and chemical degradation in field aged transformer insulation oil using spectroscopic techniques," in *Proc. Int. Conf. Diag. Electr. Eng. (Diagnostika)*, Sep. 2018, pp. 1–4.
- M. Nadj, H. Jegadeesan, A. Maedche, D. Hoffmann, and P. Erdmann, "A situation awareness driven design for predictive maintenance systems: The case of oil and gas pipeline operations," in *Proc. 24th Eur. Conf. Inf. Syst.*, 2016, pp. 1–10.
- W. Zhang, D. Yang, and H. Wang, "Data-driven methods for predictive maintenance of industrial equipment: A survey," *IEEE Syst. J.*, vol. 13, no. 3, pp. 2213–2227, Sep. 2019, doi: [10.1109/JSYST.2019.2905565](https://doi.org/10.1109/JSYST.2019.2905565).
- J. Negi and G. Maithani, "Power transformer condition assessment through insulating oil testing," in *Proc. Integr. Intell. Enable Netw. Comput. (IENC)*, Singapore: Springer, 2021, pp. 161–170.
- C. H. Tan, I. Kong, U. Irfan, M. I. Solihin, and L. P. Pui, "Edible oils adulteration: A review on regulatory compliance and its detection technologies," *J. Oleo Sci.*, vol. 70, no. 10, pp. 1343–1356, 2021.
- Q. Liu, Z. Gong, D. Li, T. Wen, J. Guan, and W. Zheng, "Rapid and low-cost quantification of adulteration content in camellia oil utilizing UV-Vis-NIR spectroscopy combined with feature selection methods," *Molecules*, vol. 28, no. 16, p. 5943, Aug. 2023, doi: [10.3390/molecules28165943](https://doi.org/10.3390/molecules28165943).
- M. Sejkorova and I. Hurtova, "Engine oil analysis-effective instrument to evaluate the reliability of tractors engines," in *Proc. 18th Int. Sci. Conf. Eng. Rural Develop.*, Jelgava, Latvia, May 2019, pp. 971–976.
- R. F. Lara, S. M. Azcarate, M. Á. Cantarelli, I. M. Orozco, M. E. Caroprese, M. Savio, and J. M. Camiña, "Lubricant quality control: A chemometric approach to assess wear engine in heavy machines," *Tribol. Int.*, vol. 86, pp. 36–41, Jun. 2015.
- F. L. Dickert, P. Forth, P. A. Lieberzeit, and G. Voigt, "Quality control of automotive engine oils with mass-sensitive chemical sensors—QCMs and molecularly imprinted polymers," *Fresenius' J. Anal. Chem.*, vol. 366, no. 8, pp. 802–806, Apr. 2000.
- Y. Zaarour, F. E. Arroud, H. Griguer, R. E. Alami, M. E. Kohen, W. Salhi, A. Faik, and M. Drissi, "The quality monitoring of paracetamol medication using a noninvasive microwave sensor," *Sci. Rep.*, vol. 13, no. 1, p. 17443, Oct. 2023, doi: [10.1038/s41598-023-43409-y](https://doi.org/10.1038/s41598-023-43409-y).
- M. E. Gharbi, M. Martínez-Estrada, R. Fernández-García, and I. Gil, "Determination of salinity and sugar concentration by means of a circular-ring monopole textile antenna-based sensor," *IEEE Sensors J.*, vol. 21, no. 21, pp. 23751–23760, Nov. 2021, doi: [10.1109/JSEN.2021.3112777](https://doi.org/10.1109/JSEN.2021.3112777).
- Y. Akazzim, C. P. Arias, M. Jofre, O. E. Mrabet, J. Romeu, and L. Jofre-Roca, "UWB microwave functional brain activity extraction for Parkinson's disease monitoring," *IEEE Sensors J.*, vol. 24, no. 3, pp. 3844–3852, Feb. 2024, doi: [10.1109/JSEN.2023.3341168](https://doi.org/10.1109/JSEN.2023.3341168).
- K. Staszek, I. Piekarz, J. Srodecki, S. Koryciak, K. Wincza, and S. Gruszczynski, "Low-cost microwave vector system for liquid properties monitoring," *IEEE Trans. Ind. Electron.*, vol. 65, no. 2, pp. 1665–1674, Feb. 2018, doi: [10.1109/TIE.2017.2733423](https://doi.org/10.1109/TIE.2017.2733423).
- S. Trabelsi and S. O. Nelson, "Microwave sensing of quality attributes of agricultural and food products," *IEEE Instrum. Meas. Mag.*, vol. 19, no. 1, pp. 36–41, Feb. 2016, doi: [10.1109/MIM.2016.7384959](https://doi.org/10.1109/MIM.2016.7384959).
- Y. Zaarour, F. Z. E. Arroud, O. E. Mrabet, A. Faik, R. E. Alami, and H. Griguer, "Real-time characterization of phosphate powder with microwave sensor: Investigating the impact of temperature," *IEEE Sensors J.*, vol. 24, no. 17, pp. 27847–27858, Sep. 2024, doi: [10.1109/JSEN.2024.3430490](https://doi.org/10.1109/JSEN.2024.3430490).
- Y. Wu, G. R. Pecorella, G. Verderame, D. Annicchiarico, T. Galhena, S. Hodge, H. J. Joyce, P. Livreri, and A. Lombardo, "Microwave gas sensor based on graphene aerogels," *IEEE Sensors J.*, vol. 23, no. 17, pp. 19282–19289, Sep. 2023.
- A. H. Allah, G. A. Eyebe, and F. Domingue, "Fully 3D-printed microfluidic sensor using substrate integrated waveguide technology for liquid permittivity characterization," *IEEE Sensors J.*, vol. 22, no. 11, pp. 10541–10550, Jun. 2022, doi: [10.1109/JSEN.2022.3170507](https://doi.org/10.1109/JSEN.2022.3170507).
- X. Zhang, C. Ruan, W. Wang, and Y. Cao, "Submersible high sensitivity microwave sensor for edible oil detection and quality analysis," *IEEE Sensors J.*, vol. 21, no. 12, pp. 13230–13238, Jun. 2021, doi: [10.1109/JSEN.2021.3067933](https://doi.org/10.1109/JSEN.2021.3067933).
- H. Xu, W.-J. Wu, W.-S. Zhao, W. Tang, and L. Sun, "Ultrasensitive edible oil sensor based on spiral SLSP combined with stepped structure," *IEEE Trans. Instrum. Meas.*, vol. 73, 2024, Art. no. 6003209, doi: [10.1109/TIM.2024.3368483](https://doi.org/10.1109/TIM.2024.3368483).
- D. M. Pozar, *Microwave Engineering: Theory and Techniques*. Hoboken, NJ, USA: Wiley, 2021.
- F. Niknahad, O. Niksan, and M. H. Zarifi, "Tunable microwave waveguide probe for noncontact ice detection on metallic surfaces," *IEEE Sensors J.*, vol. 24, no. 17, pp. 27421–27428, Sep. 2024, doi: [10.1109/JSEN.2024.3425311](https://doi.org/10.1109/JSEN.2024.3425311).
- O. Niksan, A. Shah, and M. H. Zarifi, "Waveguide iris sensor with thermal modulation for non-intrusive flow rate measurements," in *IEEE MTT-S Int. Microw. Symp. Dig.*, Denver, CO, USA, Jun. 2022, pp. 1048–1051, doi: [10.1109/IMS37962.2022.9865459](https://doi.org/10.1109/IMS37962.2022.9865459).
- J. F. da Silveira Petrucci, E. Tütüncü, A. A. Cardoso, and B. Mizaikoff, "Real-time and simultaneous monitoring of NO, NO₂, and N₂O using substrate-integrated hollow waveguides coupled to a compact Fourier transform infrared (FT-IR) spectrometer," *Appl. Spectrosc.*, vol. 73, no. 1, pp. 98–103, 2019.
- C. A. Balanis, *Antenna Theory: Analysis and Design*. Hoboken, NJ, USA: Wiley, 2016.
- A. B. Sanadi, M. Ramesh, and A. T. Kalghatgi, "Simplified design and analysis method for a waveguide iris filter," *Int. J. RF Microw. Comput.-Aided Eng.*, vol. 9, no. 2, pp. 150–154, Mar. 1999.
- S. Gabriel, R. W. Lau, and C. Gabriel, "The dielectric properties of biological tissues: III. Parametric models for the dielectric spectrum of tissues," *Phys. Med. Biol.*, vol. 41, no. 11, pp. 2271–2293, Nov. 1996.
- F. Z. E. Arroud, K. E. Fakhouri, Y. Zaarour, C. Ramdani, H. Griguer, M. Aznabet, R. E. Alami, and M. E. Bouhssini, "Thermal effect of microwave radiation on *Dactylopius opuntiae* in Morocco and coaxial probe for permittivity measurements," *IEEE Access*, vol. 12, pp. 80910–80921, 2024, doi: [10.1109/access.2024.3410161](https://doi.org/10.1109/access.2024.3410161).
- J.-Y. Shim and J.-Y. Chung, "Complex permittivity measurement of artificial tissue emulating material using open-ended coaxial probe," *IEEE Sensors J.*, vol. 20, no. 9, pp. 4688–4693, May 2020, doi: [10.1109/JSEN.2020.2966975](https://doi.org/10.1109/JSEN.2020.2966975).
- A. García, J. L. Torres, M. De Blas, A. De Francisco, and R. Illanes, "Dielectric characteristics of grape juice and wine," *Biosystems Eng.*, vol. 88, no. 3, pp. 343–349, Jul. 2004.
- K. Folgerø and T. Tjomsland, "Permittivity measurement of thin liquid layers using open-ended coaxial probes," *Meas. Sci. Technol.*, vol. 7, no. 8, pp. 1164–1173, Aug. 1996.
- M. Abdolrazzaghi, N. Katchinskiy, A. Y. Elezabi, P. E. Light, and M. Daneshmand, "Noninvasive glucose sensing in aqueous solutions using an active split-ring resonator," *IEEE Sensors J.*, vol. 21, no. 17, pp. 18742–18755, Sep. 2021, doi: [10.1109/JSEN.2021.3090050](https://doi.org/10.1109/JSEN.2021.3090050).
- P. Vélaz, L. Su, K. Grenier, J. Mata-Contreras, D. Dubuc, and F. Martín, "Microwave microfluidic sensor based on a microstrip splitter/combiner configuration and split ring resonators (SRRs) for dielectric characterization of liquids," *IEEE Sensors J.*, vol. 17, no. 20, pp. 6589–6598, Oct. 2017, doi: [10.1109/JSEN.2017.2747764](https://doi.org/10.1109/JSEN.2017.2747764).
- M. Abdolrazzaghi, M. H. Zarifi, and M. Daneshmand, "Sensitivity enhancement of split ring resonator based liquid sensors," in *Proc. IEEE Sensors*, Oct. 2016, pp. 1–3, doi: [10.1109/ICSENS.2016.7808957](https://doi.org/10.1109/ICSENS.2016.7808957).
- E. Massoni, G. Siciliano, M. Bozzi, and L. Perreggini, "Enhanced cavity sensor in SIW technology for material characterization," *IEEE Microw. Wireless Compon. Lett.*, vol. 28, no. 10, pp. 948–950, Oct. 2018, doi: [10.1109/LMWC.2018.2864876](https://doi.org/10.1109/LMWC.2018.2864876).



YOUSSEF ZAAROUR (Student Member, IEEE) received the License degree in electronics from Cadi Ayyad University, in 2018, and the M.Sc. degree in electronics and telecommunication from Abdelmalek Essaadi University, Morocco, in 2020. He is currently pursuing the Ph.D. degree with the Microwave Sensing and Energy (MSE) Department, University Mohammed VI Polytechnic (UM6P), Ben Guerir, Morocco. In 2020, he held a position as a Research Assistant with the

Information and Telecommunication Systems Laboratory (LaSIT), Faculty of Sciences, Tetouan, Morocco. He has been awarded the Erasmus + Mobility Grant and the IEEE Antennas and Propagation Society 2024 Student Travel Grant. He is also involved in monitoring biological microwave sensors. Additionally, he has actively participated in numerous conferences and has been recognized for his exceptional contributions, receiving four gold medals in different categories, including medical and agricultural applications.



JUAN LUIS CANO was born in Torrelavega, Spain, in 1979. He received the Telecommunications Engineering and Ph.D. degrees from the Universidad de Cantabria, Santander, Spain, in 2004 and 2010, respectively.

He is currently an Assistant Professor with the Universidad de Cantabria, where he focuses on the design and measurement of microwave transmitters and receivers for radio astronomy and satellite applications. His current research interests

include design and testing of low noise amplifiers in MIC and monolithic microwave integrated circuit technologies both at room and cryogenic temperatures, design of different waveguide hardware for feed networks, and the development of new technologies for efficient subsystems in multipixel microwave cameras.



TOMAS FERNANDEZ (Member, IEEE) was born in Torrelavega, Spain, in 1966. He received the M.Sc. and Ph.D. degrees in physics from the University of Cantabria, in 1991 and 1996, respectively. Since 1998, he has been an Assistant Professor of electronics for communications and RF technologies with the University of Cantabria. Since 2023, he has been the Principal of the Escuela Técnica Superior de Ingenieros Industriales y de Telecomunicación, University of

Cantabria. He participated in several European research projects (ESPRIT No. 6050, TMR, and CABSINET) as well as in industrial RF and microwave projects with Spanish (INDRA and FAGOR S. Coop.), European companies (Siemens and Philips), and Spanish Government organizations (CIDA under KORRIGAN EDA Project). He has made contributions to high-impact publications (IEEE MTT, IEEE ED, and IEEE) as well as in international symposia (MTSS and Microwave European Conference). His research interests include large-signal non-linear modeling of III-V compound transistors and SiGe HBT's concerning the problem of the behavior dependence of such devices on thermal and frequency effects, mainly in high power GaN HEMT's. Also, he is involved in the use of components based on metamaterials for use as selective filters in receivers and transmitters at RF and microwave frequencies, as well as to detect and measure changes in the relative dielectric constant and loss tangent in liquid and solid materials. He is a Reviewer of IEEE TRANSACTIONS ON TERAHERTZ SCIENCE AND TECHNOLOGY, IEEE TRANSACTIONS ON ELECTRON DEVICES, IEEE TRANSACTIONS ON MICROWAVE THEORY AND TECHNIQUES, IEEE ELECTRON DEVICE LETTERS, *International Journal of Electronics and Communications* (Elsevier), *Microelectronic Engineering* (Elsevier), *PIER*, and *IET Circuits, Devices and Systems*.



FATIMA ZAHRAE EL ARROUD (Student Member, IEEE) received the License degree in electronics and the M.Sc. degree in telecommunication systems engineering from Abdelmalek Essaadi University, Tetouan, Morocco, in 2018 and 2020, respectively. She is currently pursuing the Ph.D. degree with the Department of Microwave Energy Sensing (MES), Digital Innovation Center of Excellence (DICE), University Mohammed VI Polytechnic, Ben Guerir, Morocco. In 2020, she

held a position as a Research Assistant with the Information and Telecommunication Systems Laboratory (LaSIT), Faculty of Sciences, Tetouan.



ABDESSAMAD FAIK received the Ph.D. degree from the University of the Basque Country, Leioa, Spain. After the Ph.D. degree, he obtained a Postdoctoral Fellowship from the CEMTHI Laboratory, CNRS, Orléans, France. He then was the Guest Scientist of German Aerospace Centre (DLR), Stuttgart, Germany. Finally, he joined CIC energiGUNE, Vitoria, Spain, as the Team Leader of the materials development and corrosion study, coordinating the activities of the researchers

within the research projects. He is currently the Director of the Laboratory of Inorganic Materials for Sustainable Energy Technologies (LIMSET). He has published over 107 peer-reviewed articles, six international patents, and presented over 100 contributions to international conferences.



RAFIQ EL ALAMI received the Engineering degree from École Mohammadia d'Ingenieurs, and the joint M.B.A. degree from UM6P/Columbia University. He is currently the Director of the Digital Innovation Center of Excellence (DICE), DICE is a center that collaborates with all UM6P's departments to apply digital technologies (big data, AI, crowd sourcing, and mobility) to accelerate research and innovation. Before joining UM6P, he has spent 18 years in different

management positions with Microsoft, USA.



HAFID GRIGUER (Member, IEEE) received the master's degree from the University of Metz, in 2005, and the Ph.D. degree in microelectronics from the National Institute of Applied Sciences, Rennes, in 2010. His work spans digital industrialization, developing innovative sensor, and microwave antenna concepts for industrial and medical use. He is currently the Vice Director of the Digital Innovation Center of Excellence (DICE), University Mohammed VI Polytechnic (UM6P), Morocco. He is an inventor holding multiple patents and has authored numerous articles and book chapters. He is a member of IEEE, contributing significantly to the field of electronic systems engineering.

...